Talanta 86 (2011) 400–407

Contents lists available at SciVerse ScienceDirect

Talanta

journal homepage: www.elsevier.com/locate/talanta

Highly sensitive amperometric detection of bilirubin using enzyme and gold nanoparticles on sol–gel film modified electrode

Palanisamy Kannan[a], Hailan Chen[a], Victor Tswen-Wen Lee[b], Dong-Hwan Kim[a,*]

[a] School of Chemical and Biomedical Engineering, Nanyang Technological University, 70 Nanyang Drive, Singapore 637457, Singapore
[b] Yong Loo Lin School of Medicine, Department of Surgery, National University of Singapore, 1E Kent Ridge Road, Singapore 119228, Singapore

ARTICLE INFO

Article history:
Received 25 July 2011
Received in revised form
19 September 2011
Accepted 20 September 2011
Available online 28 September 2011

Keywords:
Gold nanoparticles
Self-assembly
Amperometry
Bilirubin
Blood serum

ABSTRACT

We describe the development of a simple and highly sensitive electrochemical (amperometric) sensing of bilirubin based on bilirubin oxidase (BOx) incorporated into the gold nanoparticles (AuNPs). This nanoelectrode platform with self-assembled enzyme is highly sensitive toward the electrochemical oxidation of bilirubin and increased the bilirubin concentration linearly from 1 to 5000 μM with a correlation coefficient of 0.9960, and an apparent Michaelis constant ($K_{M,app}$) of 44 ± 0.4 μM. Using an amperometric method, the detection limit for bilirubin at the enzyme-modified electrode was 1.4 nM (signal-to-noise ratio = 3). The modified electrode retained a stable response for 2 days while losing only ca. 3.4% of its initial sensitivity during a 10 days storage period in 0.2 M phosphate buffer solution (pH = 8.4) at ≤4 °C. The practical application of the modified electrode was demonstrated by measuring the concentration of bilirubin in blood serum sample.

1. Introduction

Bilirubin is a tetrapyrrole compound that is formed from the breakdown of heme in red blood cells and presents in the blood as an unconjugated (free) form [1–3]. Normally, it is conjugated with albumin to form a water-soluble complex and is excreted from hepatocytes into bile mainly as bilirubin glucuronides [4–6]. Bilirubin is rarely excreted from urine in its true form, but with liver dysfunction, conjugated bilirubin can be excreted with urine which is a symptom of clinical jaundice [1,4–6]. Normal levels of bilirubin in blood serum of adult range from 10^{-5} M to 10^{-6} M [1]. When the amount of bilirubin in the body exceeds the binding capacity of albumin, extra free bilirubin binds and deposits to various tissues, especially in the brain with deleterious effects [1,4–6]. Its deposition and accumulation in tissues can cause disorders in the metabolism of bilirubin and lead to hepatitis, jaundice or kernicterus [7–9]. This may cause cell death in various tissues and possibly lead to brain neuron damage causing mental disorder (e.g., mental retardation, learning disability and deafness), cerebral palsy or even death (especially in the case of babies) [9–11]. Neonatal jaundice is extremely common as almost every newborn develops an unconjugated serum bilirubin level of >30 μmol/L during the first week of life, and is reportedly more common in East Asians [12]. Transcutaneous bilirubinometry which is portable and non-invasive cannot be relied on for accurate measurements of serum bilirubin in infants with jaundice and can be only used as a screening tool [13]. Thus, the accurate determination of bilirubin is clinically important.

In the past few years, numerous methods have been developed for the detection of bilirubin in clinical samples and the most common detection methods are the direct spectroscopic measurement [14] and the diazo reaction [15]. However, the direct spectroscopic measurement of bilirubin suffers from the interference from other heme proteins and the accuracy in determination of the bilirubin concentration based on diazo reaction is compromised, partly as the reaction rate is pH dependent [16]. Other analytical methods, such as polarography [17] and fluorometry [18] have also been well known for the bilirubin detection analysis. These methods are also less selective compared to the diazo reaction [15]. Alternatively, there have been extensive attempts to obtain more accurate and simple routine analytical methods [19–21] including various enzymatic systems for the determination of bilirubin in analytical electrochemistry [22–29]. Importantly, the high over-potential required for oxidation is a major concern with electrochemical methods while using multilayered, polymer film–Mn(II) complex and AuNPs–MWCANT modified electrodes. For instance, the oxidation of bilirubin occurred at 0.6, 0.4 and 0.45 V for multilayered, polymer film–Mn complex and AuNPs–MWCNT modified electrodes, respectively [23,28,29]. Sensitivity of the enzyme electrode mainly depends on the number of bilirubin oxidase layers attached

* Corresponding author. Tel.: +65 6790 4111; fax: +65 6791 1761.
E-mail address: dhkim@ntu.edu.sg (D.-H. Kim).

0039-9140/$ – see front matter © 2011 Elsevier B.V. All rights reserved.
doi:10.1016/j.talanta.2011.09.034

to the electrode surface, further the amperometric current response was negligible at high blood serum concentration [23] and the stability of AsOx largely depends on the PEI coating in the case of polymer-coated electrode [28]. Thus, the development of a simple and highly sensitive detection platform for the determination of bilirubin is much needed.

The sol–gel technology provides a versatile way to prepare a 3-D silicate network through the hydrolysis and condensation of silicon alkoxide precursors [30]. The sol–gel-derived three-dimensional (3-D) network is particularly attractive in the development of sensing devices [31–34], because the network exhibits tunable porosity, high thermal stability and chemical inertness. Gold nanoparticles (AuNPs) have emerged as a promising nanomaterial and their widespread applications in the fields of electronics, catalysis and biosensors [35–43]. In the recent past AuNPs-based materials have been used for the immobilization of enzymes such as ascorbate oxidase, glucose oxidase, alcohol dehydrogenase and bilirubin oxidase for the development of biosensors [44–49] and biofuel cell [50] applications. In the present investigation, the AuNPs platform can provide a suitable environment for the self-assembling of BOx enzyme and the enzyme/nanoparticles based biosensing electrode displays excellent performance in terms of operating potential, detection limit, stability and reproducibility with respect to the existing enzyme, polymer and nanomaterials based electrodes.

2. Experimental

2.1. Chemicals

Bilirubin, bilirubin oxidase (bilirubin:oxygen oxidoreductase, EC 1.3.3.5, lyophilized powder, 17 units/mg) from *Myrothecium verrucaria,* hydrogen tetrachloroaurate trihydrate ($HAuCl_4{\cdot}3H_2O$), (3-mercaptopropyl)-trimethoxysilane (MPTS) and blood serum sample were purchased from Sigma–Aldrich. All other chemicals used in this investigation were of analytical grade and were used without further purification. The 0.2 M phosphate buffer solution (PBS, pH = 8.4) was prepared from Na_2HPO_4 and NaH_2PO_4 and a freshly prepared solution of bilirubin was used in all the experiments. Double-distilled water was used to prepare all the experimental solutions.

2.2. Instrumentation

Electrochemical measurements were performed using two-compartment, three-electrode cell with a polycrystalline Au working electrode, a Pt wire auxiliary electrode and a saturated calomel reference electrode. Cyclic voltammograms (CVs) were recorded using a computer-controlled CHI660C electrochemical analyzer (CH Instrument, USA). The electrochemical impedance measurements were performed using the BOx on AuNPs modified electrode in the presence of 1 mM of $K_3Fe(CN)_6$ in 0.2 M PBS using an alternating current voltage of 5 mV. The electrode formal potential was 0.22 V and the frequency range was from 1 Hz to 100 kHz. Scanning electron microscopic measurements were performed with a JEOL JSM-6700F field emission scanning electron microscope (FESEM). A magnetic stirrer was used to provide constant stirring during the amperometric experiment.

2.3. Preparation of colloidal gold nanoparticles (AuNPs)

All glasswares used in the following procedures were cleaned in a bath of freshly prepared 1:3 HNO_3/HCl, rinsed thoroughly with doubly distilled water and dried in hot air oven. (*Caution: aqua regia is a powerful oxidizing agent and it should be handled with extreme care*). The colloidal AuNPs were prepared by citrate reduction of $HAuCl_4$ according to the procedure described in the literature [20]. In a typical synthesis of ~12 nm-diameter AuNPs, 18.75 mg of $HAuCl_4$ in 62.5 mL of distilled water (0.88 mM) was brought to a vigorous boil with stirring in a round-bottom flask fitted with a reflux condenser and 6.5 mL of 1% (w/v) sodium citrate solution was then rapidly added to the flask. The solution was boiled for another 15 min, during which time the solution changed from pale yellow to deep red. The solution was allowed to cool to room temperature with continuous stirring. The suspension was stored at 4 °C until further use, conditions under which the nanoparticles are stable for several months. The resulting solution of AuNPs was examined using a UV–vis spectrum, which showed a strong surface plasma resonance band at 519 nm, typical characteristic feature of monodispersed AuNPs indicating that the as-synthesized AuNPs have the average diameters of ~12 nm-diameter.

2.4. Preparation of MPTS sol–gel

The MPTS sol was prepared by dissolving MPTS, methanol and water (as 0.1 M HCl) in a molar ratio of 1:3:3 and stirring the mixture vigorously for 30 min [22,46].

2.5. Self-assembling of AuNPs on MPTS sol–gel network

The polycrystalline Au electrode of geometrical surface area 0.07 cm^2 was polished repeatedly with alumina (0.06 μm) and sonicated in water for 10 min. The well-polished electrode was then subjected to electrochemical pretreatment by cycling the potential between −0.2 and 1.5 V in 0.05 M H_2SO_4 at a scan rate of 100 $V\,s^{-1}$ for 10–15 min or until a voltammogram characteristic of a clean polycrystalline Au electrode was obtained. The cleaned Au electrode was thoroughly rinsed with water and ethanol and was soaked in 0.5 mL of MPTS sol–gel for 20 min. The MPTS sol–gel chemisorbs on the polycrystalline Au electrode and exists as a 3-D silicate network [46,51]. The resulting MPTS sol–gel modified electrode was thoroughly rinsed with water to remove the physically adsorbed MPTS sol–gel and immersed into colloidal AuNP for 8 h. The thiol groups are distributed throughout the MPTS sol–gel network, the GNP can be conveniently self-assembled on the thiol groups present both inside and on the surface of the network.

2.6. Enzyme electrode preparation

6 μL of bilirubin oxidase (BOx, 50 units) in 0.2 M PBS was dispensed carefully onto the conducting surface of a freshly prepared, inverted Au/MPTS/AuNPs electrode and allowed for 2 h to dry to a film at ≤4 °C. To prevent enzyme loss, the electrode surface was carefully covered with a small eppendorf tube. The resulting modified electrode was stored at ≤4 °C in 0.2 M PBS (pH = 8.4) while not in use. Hereafter, the BOx self-assembled AuNPs will be referred to as Au/MPTS/AuNPs/BOx electrode. The amperometric biosensor for the sensing of bilirubin was fabricated as illustrated in Scheme 1. To obtain the FESEM image of the enzyme assembly on the AuNPs, a MPTS sol–gel film modified on the gold coated silicon wafer (cover slip) was used instead of a polycrystalline Au electrode. All electrochemical experiments were performed in nitrogen atmosphere. The electrochemical cell was covered by the dark-emery paper to preventing the loss of enzyme activity. The PBS (0.2 M, pH = 8.4) was used as a supporting electrolyte in all biosensor experiments. All the experiments were repeated at least four times and reproducible results were obtained. The calibration plots for the amperometric

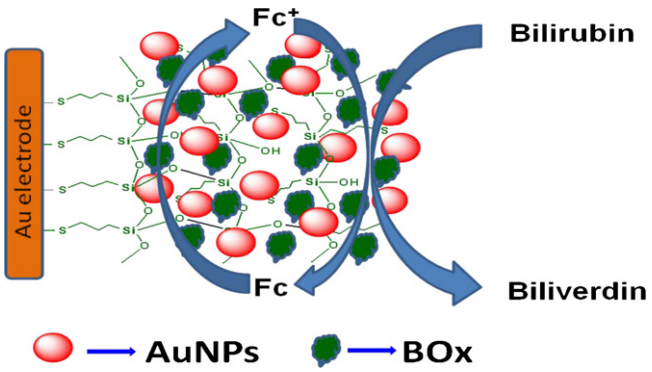

Scheme 1. Schematic representation of the oxidation of bilirubin occurred at Au/MPTS/AuNPs/BOx modified electrode.

sensing of bilirubin was made from four independent measurements.

3. Results and discussion

3.1. Characterization of BOx on AuNPs on MPTS sol–gel network

The size of the AuNPs on the MPTS sol–gel network and the surface morphology of the self-assembly of the enzyme (BOx) and AuNPs have been examined by FESEM. Fig. 1 shows the FESEM image obtained for the citrate stabilized AuNPs and the self- assembly of BOx on AuNPs. The AuNPs on the MPTS network, a size of ~12 nm in diameter and almost spherical in shape, are randomly distributed throughout the network (Fig. 1A). When BOx was assembled on the AuNP-modified gold-coated silicon wafer, aligned bright, island-like structures formed by assembling of globular BOx molecules on the AuNP cluster surfaces were observed (Fig. 1B). The AuNPs on the MPTS network greatly increase the active surface area for high BOx loading.

The distribution of both nanoparticles and the enzyme in the network facilitate the access of the substrate and result in a fast amperometric response. The observed result is consistent with the previously reported enzyme integrated assembly of AuNPs [46]. The FESEM image of the enzyme immobilized electrode confirms the existence of both nanoparticles and enzymes. Further, the self-assembly of BOx on AuNPs/MPTS modified electrode can also be monitored from the redox reaction of $[Fe(CN)_6]^{3-/4-}$ see Figs. S1 and S2.

3.2. Electrochemical oxidation of bilirubin

The main objective of the present study is to determine the concentration of bilirubin using Au/MPTS/AuNPs/BOx modified electrode. The electrochemical behaviors of the modified electrodes were investigated by CV. Fig. 2A shows the CV responses for 0.25 mM bilirubin recorded at bare Au, Au/MPTS, Au/MPTS/AuNPs and Au/MPTS/AuNPs/BOx electrodes in 0.2 M PBS (pH = 8.4) containing 0.25 mM ferrocene (Fc) as redox mediator (*vide infra*). The bare Au electrode showed an ill-defined oxidation peak in the absence of bilirubin (curve a), with formal potential $E_0' = (E_{pa} + E_{pc})/2$ at 0.08 V (versus SCE) was observed, which was assigned to one-electron reversible redox reaction of Fc^+/Fc. Addition of 0.25 mM bilirubin to the above solution, no appreciable change in the oxidation was observed (dashed line). This indicates that bare Au electrode was failed to oxidize the bilirubin. On the other hand, no oxidation peak was observed at Au/MPTS modified electrode (curve b) due to the formation of compact MPTS sol–gel film on Au electrode using the same working potential window. Interestingly, AuNPs modified electrode showed a well-defined reversible redox wave in the absence of bilirubin with formal potential E_0' at 0.06 V (versus SCE), (curve c) which was assigned to one-electron reversible redox reaction of Fc^+/Fc. After the addition of 0.25 mM bilirubin to the same solution, a slight decrease in the oxidation current was observed (dotted line). It is worth mentioning that the AuNPs are highly negative charged species as a result of the absorption of citrate ion in the fabrication process and they repulse the negatively charged carboxylate ions present on the bilirubin molecule and interfere with the diffusion of bilirubin toward the electrode surface. Electrochemical oxidation of bilirubin by the Au/MPTS/AuNPs/BOx electrode was then examined in the presence of Fc, which acted as an electron transfer mediator, a reversible redox reaction of the ferrocene compound was observed in the absence of bilirubin (Fig. 2B; curve d). It was an interesting to note that although electrical communication between bilirubin and the electrode is blocked by the BOx [23], the electrochemical oxidation of Fc clearly occurs. The AuNPs modified electrode efficiently catalyzes the oxidation of Fc and it was diffusionally mediates the oxidation of BOx active site, which, in turn, oxidizes bilirubin (Scheme 1). In the presence of bilirubin to the electrolyte containing Fc, a significant increase in the anodic current was observed at 0.23 V (Fig. 2B; curve e). This increase in the anodic current might be attributed to the bio-electrocatalyzed oxidation of bilirubin, mediated by the Fc^+/Fc couple. In addition, the BOx on the AuNPs surface efficiently decreases the oxidation

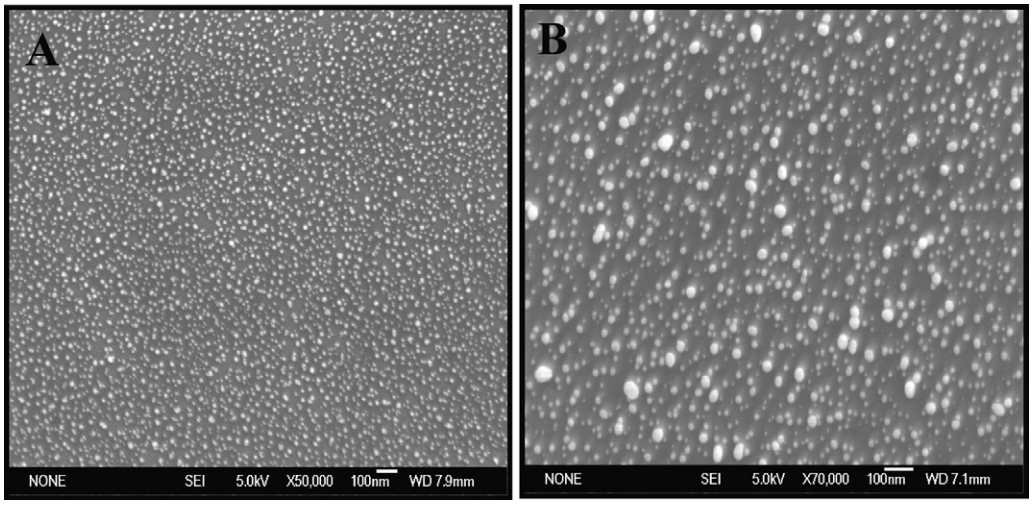

Fig. 1. FESEM images obtained for (a) citrate stabilized AuNPs and (b) self-assembly of enzyme BOx on the AuNPs/MPTS sol–gel substrates on gold coated silicon wafer.

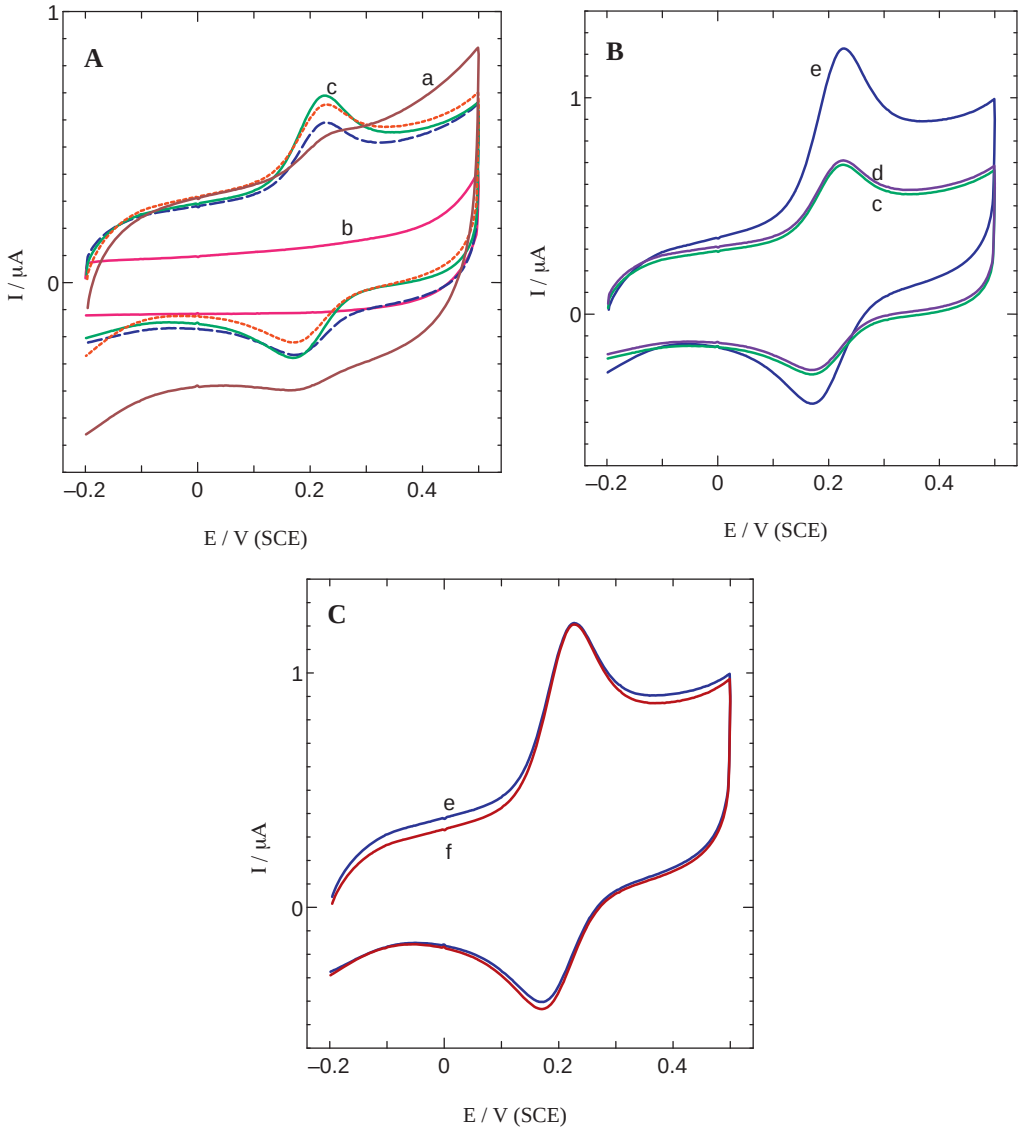

Fig. 2. (A) CVs obtained at bare Au electrode (a), Au/MPTS (b) and Au/MPTS/AuNPs (c) in the presence of 0.25 mM bilirubin in 0.25 mM Fc containing 0.20 M PBS (pH = 8.4) at a scan rate of 50 mV s^{-1}. The dashed and dotted lines for bare Au and Au/MPTS/AuNPs in the absence of 0.5 mM bilirubin. (B) CVs obtained for 0.25 mM bilirubin at the Au/MPTS/AuNPs modified electrode in the presence of 0.25 mM bilirubin (c), Au/MPTS/AuNPs/BOx modified electrode in the absence (d) and in the presence (e) of 0.25 mM Bilirubin in 0.25 mM Fc containing 0.20 M PBS (pH = 8.4). (C) CVs obtained for 0.25 mM bilirubin at the Au/MPTS/AuNPs/BOx modified electrode before (e) and after 38 ± 0.5 °C (f) in 0.25 mM Fc containing 0.20 M PBS (pH = 8.4).

over-potential about ~0.22 V less positive potential, when compared to the previous reports [28,52]. The significant decrease in the over-potential associated with a considerable increase in the anodic peak current reflects a faster electron-transfer reaction on the enzyme/nanoparticles platform owing to the high electrocatalytic effect of the BOx on the AuNPs. Further, to understand the fast electron transfer reaction of bilirubin at Au/MPTS/AuNPs/BOx modified electrode quantitatively, we have calculated the standard heterogeneous rate constant (k_s) for bilirubin at Au/MPTS/AuNPs/BOx, Au/MPTS/AuNPs and bare Au electrodes using Velasco equation [53] as given below.

$$k_s = 1.11\, D_o^{1/2}(E_p - E_{p/2})^{-1/2}\nu^{1/2}$$

where, k_s is standard heterogeneous rate constant; D_o is apparent diffusion coefficient; E_p is oxidation peak potential; $E_{p/2}$ is half-wave oxidation peak potential and ν is the scan rate. In order to determine the k_s it is necessary to find the diffusion coefficient for bilirubin. The D_o value was determined by a single potential chronoamperometry technique based on the Cottrell slope [54]. The estimated k_s values for the oxidation of bilirubin at bare Au, Au/MPTS/AuNPs and Au/MPTS/AuNPs/BOx modified electrodes were found to be 2.18×10^{-2}, 2.80×10^{-2} and 3.75×10^{-2} cm s^{-1} respectively. The obtained higher k_s value for bilirubin at Au/MPTS/AuNPs/BOx modified electrode indicated that the oxidation of bilirubin was faster than at Au/MPTS/AuNPs and bare Au electrodes.

Further, we have investigated whether the oxidation of bilirubin at Au/MPTS/AuNPs/BOx modified electrode is due to diffusion control or adsorbed species by varying the scan rates. The oxidation peak current of bilirubin increased when the scan rate was increased, as shown in Fig. S3. A good linearity between the anodic peak current and the square root of the scan rate with a correlation coefficient of 0.9985 was obtained within the range of 25–250 mV s^{-1}. This indicated that the electrode reaction of bilirubin was under diffusion controlled process. The Au/MPTS/AuNPs/BOx electrode exhibited an enhanced electrocatalytic response to bilirubin mainly due to the following two

reasons; (i) the AuNPs can act as tiny conducting centers. They were distributed throughout the MPTS sol–gel network and formed a continuous assembly of AuNPs on the electrode, which can decrease the energy barrier, facilitate electron transfer, improve biosensor response and then enhance the catalytic activity of Box, (ii) the AuNPs have large specific surface area and produced a three-dimensional assembly of BOx, which can immobilize higher amount of enzymes as compared to the two-dimensional substrate. Furthermore, the AuNPs can provide a favorable microenvironment for the active immobilization of BOx due to their excellent biocompatibility. Another important aspect requiring consideration is the stability of the Au/MPTS/AuNPs/BOx electrode. The BOx enzyme is sensitive to the temperature and the previous study has revealed its deactivation (50% activity lost within 17 h at 37 °C) [55]. In the present study, the detection sensitivity gradually increased with the temperature (tested from 34 °C), and saturated at a maximum value of 39 °C. Above 39 °C, thermal inactivation dominates over the increase of the collision frequency, resulting in the decrease of the biosensor signal. In addition, the signals become unstable. Based on the above optimization, temperature of 38 ± 5 °C was chosen as the working temperature for our experiments. We found that the Au/MPTS/AuNPs/BOx electrode showed an unchanged voltammetric response for a period of 18 h at 38 ± 0.5 °C as shown in Fig. 2C; curve e and f. The electrocatalytic activity of the enzyme electrode declined, however, upon long term storage of the electrode in the electrolyte solution (38 ± 0.5 °C). Again the electrocatalytic activity of the enzyme electrode was nevertheless preserved when kept in ≤4 °C.

3.3. pH optimum

Given that pH is a critical determinant of enzymatic activity, the pH dependence of the maximum voltammetric current at the Au/MPTS/AuNPs/BOx electrode was measured. The pH range 6.4–10.4 in PBS containing 0.25 mM bilirubin and 0.25 mM Fc shows the oxidation current gradually increased from the pH 6.4 to 8.4 (supporting information Fig. S4). The oxidation current decreased slowly as the pH increased over 8.4. This result is in good correlation to the maximum activity of BOx at pH = 8.4 given in the literature [56]. Thus, the AuNPs modified sol–gel matrix did not change the optimal pH value for the bioelectrocatalytic reaction of the immobilized BOx toward the oxidation of bilirubin. The optimum pH = 8.4 was (in PBS) showed the good sensitivity toward bilirubin detection using Au/MPTS/AuNPs/BOx electrode, so this combination was chosen for all electrochemical measurements.

3.4. Amperometric determination of bilirubin

The sensitivity of Au/MPTS/AuNPs/BOx modified electrode to bilirubin was analyzed by using constant potential amperometry under steady-state conditions. Fig. 3A depicts the amperometric *i–t* curve obtained for the oxidation of bilirubin at the Au/MPTS/AuNPs/BOx modified electrode in a constantly stirred 0.2 M PBS containing 0.25 mM Fc at an applied potential of +0.35 V. An initial steady-state amperometric current response was observed due to the addition of 1 μM bilirubin and then the addition of 1 μM bilirubin in each step with a sample interval of 50 s, the current response linearly increases and a steady state current response was obtained within 2 s which indicates a fast electron-transfer process at this electrode. We found that 14 nA current was obtained for single addition of 1 μM bilirubin at Au/MPTS/AuNPs/BOx electrode. The observed stable amperometric current response with higher sensitivity of bilirubin at Au/MPTS/AuNPs/BOx modified electrode indicated that this electrode can be successfully used for the sensitive detection of 1 μM bilirubin. Further, we have studied the response of the enzyme-modified electrode as a function of bilirubin concentrations (at pH = 8.4) are shown in Fig. 3B. The catalytic oxidation current at +0.35 V versus Ag/AgCl depends linearly on bilirubin concentrations in the range of 1–5000 μM with a correlation coefficient of 0.9960 and the detection limit calculated from the standard deviation of the baseline current as described [57] was found to be 1.4 nM (S/N = 3). We have also calculated the apparent Michaelis constant [58] ($K_{M,app}$, equ. given below) value and was found to be 44 ± 0.4 μM.

$$i_{\text{lim}} = \frac{i_{\max}[\text{bilirubin}]}{K_{M,app} + [\text{bilirubin}]}$$

where $i_{\max}$ is the saturation limiting current and $K_{M,app}$ is the apparent Michaelis constant. To the best of our knowledge, this is the first time such a very low detection limit (1.4 nM) has been achieved by the electrochemical method.

It is worth comparing the analytical performance of the Au/MPTS/AuNPs/BOx modified electrode with those of available enzyme, polymer-composite and other chemically modified

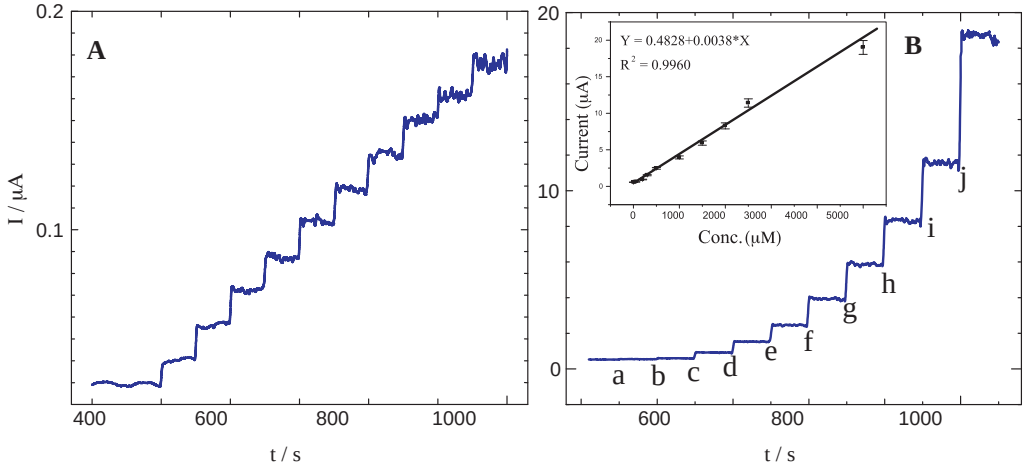

Fig. 3. (A) Amperometric *i–t* curve obtained for the determination of bilirubin at the Au/MPTS/AuNPs/BOx modified electrode in 0.25 mM Fc containing 0.20 M PBS (pH = 8.4). Each addition increases the concentration of bilirubin 1 μM at a regular interval of 50 s. E_{app} = +0.35 V. (B) Amperometric *i–t* curve for the determination of bilirubin at the Au/MPTS/AuNPs/BOx modified electrode in 0.20 M PB solution. Each addition increases the concentration of bilirubin: (a) 1, (b) 50, (c) 200, (d) 300, (e) 500, (f) 1000, (g) 1500, (h) 2000, (i) 2500 and (j) 5000 μM at a regular interval of 50 s. E_{app} = + 0.35 V. The inset is corresponding calibration plot obtained for amperometric current vs. concentrations of bilirubin.

Table 1
Comparison of detection limit at the present modified electrode with the reported materials and chemically modified electrodes.

S. No.	Modified materials	Operation potential	linear rage (μM)	Stability (in days)	Detection limit (μM)	Reference
1	Fiber optic senor based on fluorescence quenching of [Ru(dpp)$_3$]	–	1×10^{-7}–3×10^{-4}	20	0.05	[16]
2	Multilayered enzyme electrode	V	1×10^{-5}–1.1×10^{-4}	75	17	[23]
3	The BOx immobilized on a platinum electrode	–	1×10^{-6}–3×10^{-4}	30	0.7	[24]
4	The BOx enzyme cross linking with BSA and glutaraldehyde on pre-activated membrane	–	1×10^{-5}–2.5×10^{-4}	30	8	[25]
5	Poly-TTCA–Mn(II)/PEI–AsOx on GC electrode	V	1×10^{-7}–5×10^{-5}	60	0.04	[28]
6	Ferrocenecarboxamide modified MWCNT/AuNPs electrode	V	1×10^{-6}–1×10^{-4}	30	0.12	[29]
7	Incorporation of bilirubin oxidase (BOx) and HRP within a graphite-epoxy matrix	–	4×10^{-6}–1×10^{-4}	–	4	[52]
8	BOx/AuNPs/MPTS electrode	V	1×10^{-6}–5×10^{-3}	80	0.0023	This work

electrodes (Table 1). A detection of 50 nM was bilirubin achieved by fiber optic senor based on fluorescence quenching of tris(4,7-diphenyl-1,10-phenanthroline) ruthenium chloride, [Ru(dpp)$_3$][16]. Wang and Ozsoz reported the detection of 4 μM based on amperometric enzyme electrode for bilirubin biosensor [52]. Karayannis and co-workers reported the detection limit of 8 μM based on indirect electrochemical monitoring of bilirubin via its reaction with oxygen to biliverdin in the presence of BOx [25]. Fortuney and Guilhault reported the detection limit of 0.7 μM using BOx immobilized on platinum electrode [24]. Recently, Shim and co-workers reported the detection limit of 40 nM of bilirubin biosensor using poly-TTCA–Mn(II)/PEI–AsOx electrode [28]. However, Au/MPTS/AuNPs/BOx modified electrode could successfully detect bilirubin even in the presence of interferents (*vide infra*) indicating that the analytical performance of the Au/MPTS/AuNPs/BOx electrode is superior to that of reported electrodes.

3.5. Effect of interferents

To demonstrate the selectivity of the proposed biosensor, we have studied the determination of bilirubin in the presence of several interferents of typical bio-organic compounds, such as dopamine, glucose, ascorbic acid and uric acid by amperometric method. Fig. S5 in supporting information shows the amperometric *i*–*t* curve obtained for bilirubin at Au/MPTS/AuNPs/BOx modified electrode in the presence of several interferents in a constantly stirred 0.2 M PBS (pH = 8.4) containing 0.25 mM Fc at a constant applied potential of 0.35 V. The initial addition was due to 0.5 mM each dopamine (a), glucose (b), ascorbic acid (c) and uric acid (d) separately with a sample interval of 50 s to the same 0.2 M PBS, no noticeable change in amperometric current response was observed. However, the addition of 1 μM bilirubin to the same solution (e, f and g), the current response was increased rapidly due to the higher affinity of BOx modified electrode toward the bilirubin. This result indicates that Au/MPTS/AuNPs/BOx electrode can be successfully used for the determination of 1 μM bilirubin even in the presence of 500-fold excess of several interferents including neurotransmitter compound.

3.6. Stability and reproducibility

Stability of the electrode is very important for practical biosensing applications. The enzyme modified AuNPs electrode was very stable when it was kept in 0.2 M PBS (pH = 8.4). The reproducibility of the four different sets of enzyme modified AuNPs electrodes were examined by a series of 40 successive cyclic votammetric measurements for 0.25 mM bilirubin in 0.2 M PBS (pH = 8.4). The relative standard deviation was found to be 1.2%, indicating that the modified electrodes have good stability and repeatability within a confidence level of 96%, suggesting that the electrodes are highly stable during the CV measurements. Very recently, Shim and co-workers [28] have reported the RSD of 5.3% for bilirubin at polyTTCA–Mn(II)/PEI–AsOx electrode and Karayannis and co-workers reported the RSD of 3.1% for Bilirubin [25]. A 3.8% RSD value was reported by Fortuney and Guilhault using BOx immobilized on platinum electrode [24] and 14% RSD value was reported by Wang and Ozsoz using an amperometric enzyme electrode modified with BOx and horseradish peroxidase [52]. To check the long-term storage stability of the present bilirubin sensor, the Au/MPTS/AuNPs/BOx electrode was kept in 0.2 M PBS (pH = 8.4) at ≤4 °C. No appreciable decrease in the oxidation current response of bilirubin was observed for two days and the current decreased by only 3.4% after 10 days (Fig. S6) and retained 93% of its initial response of bilirubin oxidation more than 2 months. To ascertain the reproducibility of the results, two different Au electrodes were modified with the MPTS/AuNPs/BOx in the same way and the each electrode's response toward 0.25 mM bilirubin was tested by four repeat measurements. The peak current obtained in the four repeat measurements of two independent electrodes again showed an RSD of 1.8%, confirming that the results are highly reproducible.

3.7. Real sample analysis

In order to verify the performance and feasibility of the method for analysis of bilirubin in real sample, the proposed electrode was applied to the determination of bilirubin in blood serum sample (calibrated result; 50 μL of blood serum sample contains 1.6–1.9 μM of bilirubin). Fig. 4 is the DPV response obtained for the real sample. The 50 μL real sample (blood serum sample) was injected into the supporting electrolyte in each step increments and voltammograms were recorded with the optimized parameters in presence of nitrogen atmosphere. As shown, gradual increase in the current due to bilirubin (~0.18 V) was observed upon the addition of blood serum sample, demonstrating that the Au/MPTS/AuNPs/BOx electrode is potentially useful for detection of bilirubin in the blood sample analysis. Furthermore, a small broad peak (~0.03 V) was ascribed due to the oxidation of ascorbic acid in the blood serum sample. The results were listed in Table 2. The recovery results were acceptable, showing that the proposed methods could be efficiently used for the determination of bilirubin in real sample. Further, the concentration of bilirubin was obtained from the standard calibration plot and was 1.8 ± 0.1 μM, which is significantly improved detection than the recent report on the bilirubin level in the blood serum [28].

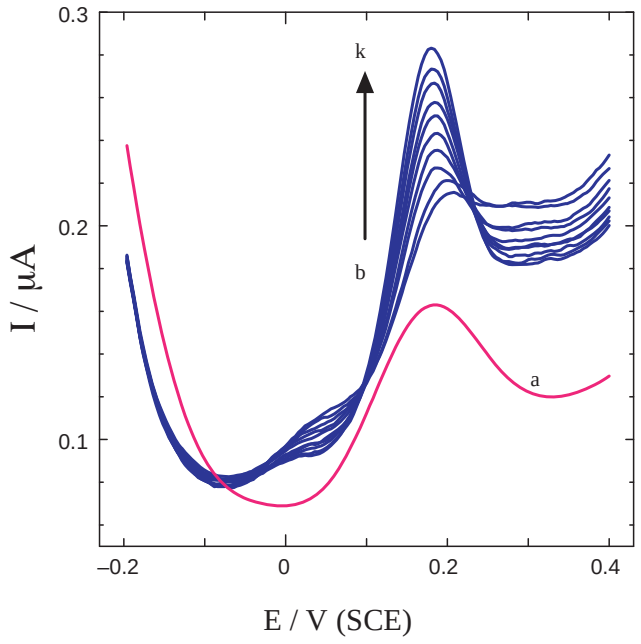

Fig. 4. DPVs obtained for 0.25 mM Fc containing 0.20 M PBS (pH = 8.4) in the absence (a) and presence of 50 μL of blood serum sample (b–k) at Au/MPTS/AuNPs/BOx modified electrode.

Table 2
Results of detection after spiking the blood serum sample into the 0.2 M PBS (pH = 8.4).

S. No.	Standard spike of blood serum sample (μL)	Bilirubin detected after spike (μM)	Recovery (%)
1	50	1.6	84
2	50	1.7	89
3	50	1.6	84
4	50	1.8	94
5	50	1.8	94
6	50	1.7	89
7	50	1.6	84
8	50	1.8	94
9	50	1.7	89
10	50	1.6	84

4. Conclusions

The development of a simple and highly sensitive electrochemical (amperometric) bilirubin biosensor based on BOx incorporated AuNPs is described. This enzyme self-assembled AuNPs platform is highly sensitive toward the electrochemical oxidation of bilirubin and increased the bilirubin concentration linearly from 1 to 5000 μM with a correlation coefficient of 0.9960 and an apparent Michaelis constant ($K_{M,app}$) of 44 ± 0.4 μM. Using an amperometric method, the low detection limit for bilirubin at the enzyme-modified electrode was 1.4 nM (S/N = 3). The modified electrode retained a stable response for 2 days while losing only ca. 3.4% of its initial sensitivity during a 10 days storage period in 0.2 M PBS at ≤4 °C. The practical application of the modified electrode was demonstrated by measuring the concentration of bilirubin in blood serum samples.

Acknowledgments

This work was financially supported by the Academic Research Funding Tier 1 (RG65/08) and the National Medical Research Council (NMRC/NIG/00602009) of Singapore.

Appendix A. Supplementary data

Supplementary data associated with this article can be found, in the online version, at doi:10.1016/j.talanta.2011.09.034.

References

[1] T.K. With, Bile Pigments, Chemical Biological and Clinical Aspects, Academic Press, New York, 1968.
[2] J.D. Ostrow, Bile Pigments and Jaundice: Molecular, Metabolic and Medical, M.D. Aspects, Marcel Dekker Inc, New York, 1986.
[3] M.E. Avramescu, W.F.C. Sager, Z. Borneman, M. Wessling, J. Chromatogr. B 803 (2004) 215–223.
[4] X. Wang, J.R. Chowdhury, N.R. Chowdhury, Curr. Paediatr. 16 (2006) 70–74.
[5] Y. Andreu, M. Ostra, C. Ubide, J. Galbán, S. de Marcos, J.R. Castillo, Talanta 57 (2002) 343–353.
[6] W. Gaoming, G.R. Brown, React. Polym. 14 (1991) 49–61.
[7] M.M. Khan, S. Tayyab, Biochim. Biophys. Acta Protein Struct. Mol. Enzymol. 1545 (2001) 263–277.
[8] T. Hargreaves, The Liver and Bile Metabolism, Appleton-century-crofts, New York, 1968.
[9] M.J. Maisels, in: G.B. Avery (Ed.), Neonatology, Pathophysiology and Management of the Newborn, Lippincott Williams & Wilkins, Philadelphia, 1989.
[10] S.M. Shapiro, Pediatr. Neurol. 29 (2003) 410–421.
[11] M. Kaplan, C. Hammerman, Clin. Chim. Acta 356 (2005) 9–21.
[12] S. Linn, S.C. Schoenbaum, R.R. Monson, B. Rosner, P.G. Stubblefield, K.J. Ryan, Pediatrics 75 (1985) 770–774.
[13] S. Samanta, M. Tan, C. Kissack, S. Nayak, R. Chittick, C.W. Yoxall, Acta Paediatr. 93 (2004) 1486–1490.
[14] B.T. Doumas, B.W. Perry, E.A. Sasse, J.V. Straumfjord Jr., Clin. Chem. 19 (1973) 984–993.
[15] H.U. Bergmeyer, Methods of Enzymatic Analysis, vol. 8, 3rd ed., VCH, Weinheim, 1985, pp. 591–598.
[16] X. Li, Z. Rosenzweig, Anal. Chim. Acta 353 (1997) 263–273.
[17] J. Wang, D.B. Luo, P.A.M. Farias, J. Electroanal. Chem. Interfacial Electrochem. 185 (1985) 61–71.
[18] T.R. Koch, O.O. Akingbe, Clin. Chem. 27 (1981) 1295–1299.
[19] L.P. Palilis, A.C. Calokerinos, N. Grekas, Anal. Chim. Acta 333 (1996) 267–275.
[20] N. Nath, A. Chilkoti, Anal. Chem. 76 (2004) 5370–5378.
[21] K. Kurosaka, S. Senba, H. Tsubota, H. Kondo, Clin. Chim. Acta 269 (1998) 125–136.
[22] C.J. Brinker, G.W. Scherer, Sol–Gel Science, Academic Press, New York, 1990.
[23] B. Shoham, Y. Migron, A. Riklin, I. Willner, B. Tartakovsky, Biosens. Bioelectron. 10 (1995) 341–352.
[24] A. Fortuney, G.G. Guilbault, Electroanalysis 8 (1996) 229–232.
[25] J. Klemm, M.I. Prodromidis, M.I. Karayannis, Electroanalysis 12 (2000) 292–295.
[26] C.-Y. Huang, M.-J. Syu, Y.-S. Chang, C.-H. Chang, T.-C. Chou, B.-D. Liu, Biosens. Bioelectron. 22 (2007) 1694–1699.
[27] M.-J. Syu, T.-C. Chiu, C.-Y. Lai, Y.-S. Chang, Biosens. Bioelectron. 22 (2006) 550–557.
[28] M.A. Rahman, K.-S. Lee, D.-S. Park, M.-S. Won, Y.-B. Shim, Biosens. Bioelectron. 23 (2008) 857–864.
[29] C. Wang, G. Wang, B. Fang, Microchim. Acta 164 (2009) 113–118.
[30] L.L. Hench, J.K. West, Chem. Rev. 90 (1990) 33–72.
[31] J. Wang, P.V.A. Pamidi, Anal. Chem. 69 (1997) 4490–4494.
[32] M.M. Collinson, Acc. Chem. Res. 40 (2007) 777–783.
[33] X. Liu, W. Niu, H. Li, S. Han, L. Hu, G. Xu, Electrochem. Commun. 10 (2008) 1250–1253.
[34] P. Kannan, S.A. John, Anal. Chim. Acta 663 (2010) 158–164.
[35] P. Kannan, S.A. John, Electrochim. Acta 56 (2011) 7029–7037.
[36] N.L. Rosi, C.A. Mirkin, Chem. Rev. 105 (2005) 1547–1562.
[37] A.N. Shipway, E. Katz, I. Willner, ChemPhysChem 1 (2000) 18–52.
[38] M.-C. Daniel, D. Astruc, Chem. Rev. 104 (2003) 293–346.
[39] C.J. Zhong, M.M. Maye, Adv. Mater. 13 (2001) 1507–1511.
[40] L. Guo, G. Chen, D.-H. Kim, Anal. Chem. 82 (2010) 5147–5153.
[41] P. Kannan, S.A. John, Electrochim. Acta 55 (2010) 3497–3503.
[42] P. Si, P. Kannan, L. Guo, H. Son, D.-H. Kim, Biosens. Bioelectron. 26 (2011) 3845–3851.
[43] L. Guo, A.R. Ferhan, K. Lee, D.-H. Kim, Anal. Chem. 83 (2011) 2605–2612.
[44] S. Zhang, N. Wang, H. Yu, Y. Niu, C. Sun, Bioelectrochemistry 67 (2005) 15–22.
[45] W. Yang, J. Wang, S. Zhao, Y. Sun, C. Sun, Electrochem. Commun. 8 (2006) 665–672.
[46] B.K. Jena, C.R. Raj, Anal. Chem. 78 (2006) 6332–6339.
[47] T. Hoshi, N. Sagae, K. Daikuhara, J.-i. Anzai, Talanta 71 (2007) 644–647.
[48] R.B. Rakhi, K. Sethupathi, S. Ramaprabhu, J. Phys. Chem. B 113 (2009) 3190–3194.
[49] U. Saxena, M. Chakraborty, P. Goswami, Biosens. Bioelectron. 26 (2011) 3037–3043.
[50] K. Murata, K. Kajiya, N. Nakamura, H. Ohno, Energy Environ. Sci. 2 (2009) 1280–1285.
[51] H.O. Finklea, in: A.J. Bard, I. Rubinstein (Eds.), Electroanalytical Chemistry, vol. 19, Marcel Dekker, New York, 1996, pp. 109–335.

[52] J. Wang, M. Ozsoz, Electroanalysis 2 (1990) 647–650.
[53] J.G. Velasco, Electroanal 9 (1997) 880–882.
[54] A.J. Bard, L.R. Faulkner, Electrochemical Methods Fundamentals and Applications, Wiley, New York, 2001.
[55] C. Sung, A. Lavin, A.M. Klibanov, R. Langer, Biotechnol. Bioeng. 28 (1986) 1531–1539.
[56] S. Murao, N. Tanaka, Agric. Biol. Chem. 45 (1981) 2383–2384.
[57] H.R. Zare, F. Memarzadeh, M.M. Ardakani, M. Namazian, S.M. Golabi, Electrochim. Acta 50 (2005) 3495–3502.
[58] M. Situmorang, D. Brynn Hibbert, J. Justin Gooding, D. Barnett, Analyst 124 (1999) 1775–1779.